CONTROL-ORIENTED MODEL VERIFICATION FOR UV PROCESSING OF COMPOSITE LAMINATE

Adamu Yebi, Beshah Ayalew, Srikanth Pilla
Clemson University - International Center for Automotive Research
4 Research Dr
Greenville, SC 29607

ABSTRACT

This paper discusses partial experimental validations of a control-oriented ultraviolet (UV) curing model for a polymer composite laminate. The model describes the coupled phenomena of UV absorption, heat transfer and cure kinetics in the laminate. First, the model parameters related to UV absorption and attenuation are determined by conducting experiments that measure UV transmission in the laminate with and without photoinitiator. Then, the parameters related to cure kinetics and heat convection constant are estimated via thermal measurements. Very close agreement is shown between predictions of the overall curing model verified via these steps and in-process thermal state measurements. Finally, as an illustration of the application of the verified curing process model for practical control scheme designs, brief discussions are included that highlight the results from model-based optimization of a layer-by-layer laminate curing process.

1. INTRODUCTION

Autoclave facilities currently represent the dominant processes for curing composites. However, they typically feature high capital costs, high energy consumption and long processing times[1]. As a result, there is a need for efficient out of autoclave (OOA) technologies for processing composites. Radiation-based technologies such as microwave, infrared, ultraviolet (UV), electron beam (EB) and X-ray are regarded as viable OOA alternatives because of their higher energy efficiency and accelerated processing times [2, 3]. Among these radiation-based processes, UV curing offers advantages of low equipment costs, low energy consumption and least hazardous radiation wavelengths[4].

Despite these advantages, the thickness of laminates that can be cured effectively by UV-radiation is limited because UV attenuates as it passes through target materials[5]. To overcome this through-cure or cure penetration problem, an approach of layer-by-layer deposition and curing of composite laminates is often adopted [1]. However, still some challenges remain such as differing material shrinkage and thermal stresses between layers due to cure level and temperature gradients across layers that leads to distortion of the end product [6]. To overcome these challenges, in our previous work[7], we proposed a stepped-concurrent layering and curing(SCC) process, where new layers are added before previous ones cure completely in such a way that there is an effective reduction of cure level deviation and thermal stress in all layers. Optimization and development of these and other processing schemes is best done via validated curing process models.

In the current paper, we discuss a set of experiments and results that closely validate a UV curing process model for a composite laminate made from glass fiber and unsaturated polyester resin. These experiments include in-process thermal and UV transmission measurements as well as post-cure hardness measurements. Using the validated process parameters and optimization algorithm developed in[7], we also include some simulation results comparing curing of a thick laminate via the SCC process with one-shot curing.

2. UV CURING PROCESS MODEL

For the process set up shown in Figure 1, a 1D fiberglass composite laminate curing model is proposed with the following three assumptions. First, a resin volume fraction factor is introduced in the process model to consider the fact that only the resin portion undergoes the photopolymerization reaction[8]. Second, the average thermal properties of the resin and the fiber are taken for the properties of the composite laminate. Third, the attenuation of UV-radiation in the resin-fiber matrix in the z-direction is modeled according to Beer Lambert's Law, where a single attenuation constant will be taken for the laminate. This essentially assumes a uniformly wetted fiberglass and resin where the refractive indices of the fiber and resin are matched.
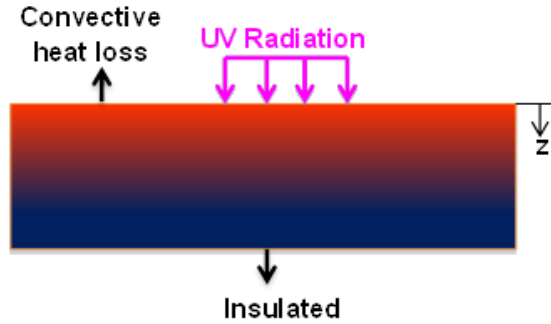

Figure 1: Schematic of a UV Curing Process

To continue with the above assumptions for more general cases, the attenuation constant for the combined resin-fiber matrix needs to be identified experimentally. In addition, for the cure kinetics model we make two changes from[7]: 1) the autocatalytic model is replaced by another autocatalytic model suggested in[9] for reasons related to numerical computations of optimality; 2) diffusion-controlled effect is added to the cure kinetics model by introducing additional parameters that account for the diffusion effect[10]. The following partial and ordinary differential equations (1-5) summarize the process model along with the boundary and initial conditions:

$$\rho c_p \frac{\partial T(z,t)}{\partial t} = \frac{\partial}{\partial z}\left(k_z \frac{\partial T(z,t)}{\partial z}\right) + v_r \rho_r \Delta H_r \frac{d\alpha(z,t)}{dt} \tag{1a}$$

$$-k_z \frac{\partial T(0,t)}{\partial z} + \vartheta I_0 = h\left(T(0,t) - T_\infty\right) \tag{1b}$$

$$\frac{\partial T(l,t)}{\partial z} = 0 \tag{1c}$$

$$\frac{d\alpha(z,t)}{dt} = S^q I_0^p \exp\left(-\lambda_c z\right) K_D(\alpha) \left[K_1(T) + K_2(T)\alpha(z,t)\right]\left(1-\alpha(z,t)\right)\left(G-\alpha(z,t)\right) \tag{1d}$$

$$T(z,0) = T_0(z) \tag{1e}$$

$$\alpha(z,0) = \alpha_0(z) \tag{1f}$$

where:

$$\lambda_c = b_r + b_{PI}S \tag{2}$$

$$K_D(\alpha) = \frac{1}{1+\exp\left(\xi\left(\alpha(z,t)-\alpha_c\right)\right)} \tag{3}$$

$$K_1(T) = A_1 \exp\left(\frac{-E_1}{RT_{abs}(z,t)}\right) \tag{4}$$

$$K_2(T) = A_2 \exp\left(\frac{-E_2}{RT_{abs}(z,t)}\right) \tag{5}$$

where ρ and c_p are the density and specific heat capacity of the composite laminate, respectively; k_z is the thermal conductivity of the laminate in the z-direction; $T(z,t)$ is temperature distribution at depth z and time t; v_r is volumetric fraction of resin in the composite matrix; ρ_r is density of resin; and ΔH_r is polymerization enthalpy of resin conversion; $E_1 \& E_2$ are activation energies, S is photoinitiator concentration, $A_1 \& A_2$ are pre-exponential rate constants; R is gas constant; I_0 is UV input intensity at the surface; $T_{abs}(z,t)$ is absolute temperature in Kelvin; $\alpha(z,t)$ is cure level/state distribution; $p \& q$ are constant exponents; b_r is absorption coefficient in the resin plus fiber without photoinitiator; b_{PI} is absorption coefficient due to photoinitiator; λ_c is the absorption coefficient in the resin plus fiber; G is constant parameter in cure kinetics; ξ is diffusion constant; α_c is critical value of cure level; ϑ is absorptivity constant of the UV radiation at the boundary; h is convective heat transfer at the top boundary; l is the thickness of a single layer, and T_∞ is constant ambient temperature; and $d\alpha(z,t)/dt$ is the rate of cure conversion (rate of polymerization).

The above listed constant parameters for the process model (1-5) are identified in three steps: 1) The UV attenuation constants ($b_r \& b_{PI}$) are determined by measuring the UV transmission through the composite laminate with and without photoinitiator; 2) The parameters related to cure kinetics $A_1, A_2, E_1, E_2 \& G$ can be extracted from Ref [10] which considered the UV curing of unsaturated polyester resins without fibers. We modified the parameters from[10] based on the temperature measurements recorded while curing composite laminate samples; 3) The model

parameters related with heat convection and conduction are identified based on a separate set of temperature measurements recorded after complete cure of the composite laminate.

3. EXPERIMENTAL VERIFICATION

3.1 Materials and Equipment

An unsaturated polyester resin (C11001-25) with 43.43% styrene content was purchased from Composite One LLC, USA. The resin contains cobalt accelerator additives mixed at a concentration of (ethylhexanoate, 12p) 0.07% and (neodecanoate, 26p) 0.009%. Usually, cobalt accelerator is added to speed up the radical formation in the presence of peroxide catalyst for the thermal curing. However, it is in general not considered necessary for UV curing. For radical photopolymerisation of the resin, 2, 2-Dimethoxy-2-phenylacetophenone was used as a photoinitiator (IRGACURE 651 by Sigma-Aldrich). E-glass (9 oz Fabric Style 7781, from Fiber Glast, USA) was used as the reinforcement fiber for the composite laminate.

A UV LED (Clearstone 42-cell, with nominal power of 16.1W) was used as the radiation source. Its UV emission peaks at wavelength of 365 nm. For measurement of the irradiance in the UV-A+B band, a digital UV radiometer (Solarmeter) was used. The minimum resolution of this instrument is 0.1 mW/cm^2. The degree of cure of the resin was quantified using surface hardness measurement. The Barcol hardness according to ASTM D 2583 can be determined by measuring the resistance of the material surface to penetration of a sharp steel point under a spring load. The depth of penetration is converted into absolute Barcol numbers on a scale from 0 to 100 (GYZJ 934 impressor). Measurement of the hardness on the top (directly exposed to irradiation) and the bottom face of the specimen allows quantification of the through-cure of the resin system. DATQ data logger from OMEGA was used to record the temperature measurement from multiple thermocouples deployed for the thermal experiments.

3.2 UV Transmission Measurement

For UV curing of a transparent medium, the UV intensity decreases exponentially as it passes more photoinitiators (PI), which absorb the UV to start the photopolymerization cure reactions. In addition to the PI, UV attenuation is also pronounced by the presence of fiber and resin. To determine the influence of the fiber and resin, the UV transmitted through laminates (resin plus fiber) with and without PI is measured.

Figure 2 shows the experimental platform for UV transmission measurement. It consists of a UV LED, glass mold (holds the resin/laminate and passes attenuated UV irradiance to sensor), and radiometer. The glass mold area is 60x100 mm and placed perpendicular to the UV line of sight at a distance of 80 mm from the surface of the UV LED. The mold is open at the top. To determine the attenuation in the glass mold alone, the UV intensity was measured with and without glass while keeping the same sensor location. The result was used to account for the effect of the mold on the intensity measurements at the bottom of the composite laminate.
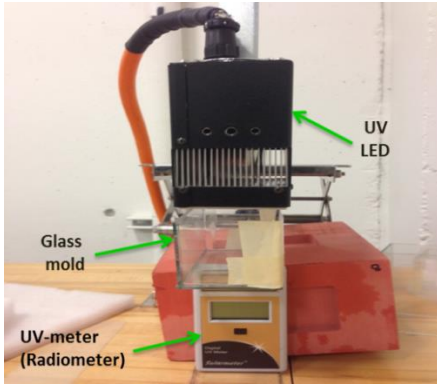
Figure 2: Experimental platform for
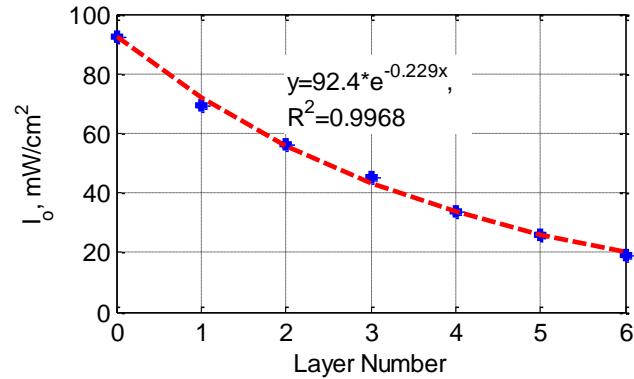UV transmission measurement

Figure 3: UV attenuation in composite laminate
layer without photoinitiator

In the first set of experiments, the UV attenuation was measured along a laminate consisting of six layers/plies with fiber to resin ratio of 40/60 % by volume. Six measurements were recorded by placing pre-preg of fiber-resin (without PI) layer-by-layer until the attenuation in all six layers is measured. Figure 3 shows the trend of UV attenuation in resin plus fiber (without PI). It is clear that, for uniformly wetted fiber plus resin, the UV attenuation follows Beer-Lambert's law. The attenuation constant is estimated to be 0.229 per layer. For resin plus fiber layer of thickness 0.35 mm (measured by micrometer), the attenuation constant in the laminate is approximately $b_r = 0.65 / mm$.

In the second set of experiments, we considered the same number of fiber plies (six) and 40/60 % by volume weight fiber to resin ratio, but with different PI concentrations of 0.05 wt%, 0.1 wt%, 0.25 wt%, 0.5 wt%, 1 wt% & 2 wt% (percentage by weight of resin). This time, the UV intensity variation with time is measured at an interval of 10 seconds at the bottom, placing all six layers once under UV exposure. The measured UV intensity for a total time length of 380 seconds is plotted in Figure 4. For all cases of PI concentrations, a good through cure is achieved for the six-layer composite laminate after 380 seconds. This is characterized by the relative hardness value measured at the top and bottom of the six-layer composite. The average hardness value at the surface of the bottom layer is more than 90 % of that of the top layer. As shown in Fig. 4, the UV intensity increases with time in the first phase of curing and starts declining thereafter. For photobleaching photoinitiators, the trend observed in the first phase of curing is expected because the resin in the top layers cures first and becomes more UV transparent to pass more UV light to the bottom layers [11]. The trend in the second phase of curing can be explained by the material degradation in the top layers because of over-curing[5]. The decrement is more pronounced for higher PI concentrations as it quickly comes to a complete cure. However, for low concentrations of PI (0.05 % & 0.1 %), the UV intensity stays constant for a long period of time after the first phase. Therefore, the UV attenuation model across depth should consider time-resolved Beer-Lambert law[11] (considering both space and time) at least for the cases of higher PI concentration(>0.1 %).
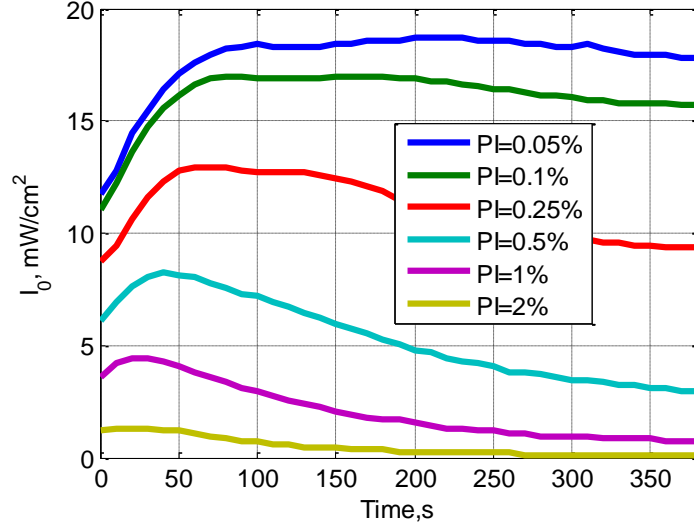
Figure 4: UV intensity at the bottom of composite laminate with time

To determine the UV attenuation constant along the depth due to PI, we considered the maximum intensity value measured for each case above. First, the average total attenuation constant (λ_c) in the composite laminate was determined in much the same way as that of attenuation constant in resin plus fiber without PI, as discussed above. Then, b_{PI} value of ($0.5/wt\% mm$) was determined using relation (2). It is interesting that the same value was determined in the related work[10], which considered the same set of PI concentrations with a similar resin type but without glass fiber.

3.3 Thermal Measurements During UV Curing of Composite Laminate

In the second phase of the experimental work, we considered the curing of the composite laminate sample (of thickness $\approx 5 mm$) to estimate some of the model parameters based on the *in-situ* temperature measurements. The composite laminate was made by hand lay-up from 15 fiber plies with 40/60 percent by weight fiber to resin ratio and with PI concentration of 0.1wt %. The laminate was cured in the insulated mold of dimension (60x100x22) mm. The insulated mold was made from polyisocyanurate foam, which is open at the top end exposed to the UV LED. The composite laminate within this insulation mold was then placed under UV source at a distance of 80 mm. It was allowed to cure for 15 minutes with a UV intensity of 100 mW/cm^2 reaching the top surface. The first set of temperature measurements was taken at the top and bottom surfaces of the laminates as the cure progressed (with K-type thermocouples). The second set of temperature measurements was taken after 15 minutes of UV curing with the UV LED turned off while the UV lamp cooling system continued working. The measurements were continued for 10 minutes until the laminate samples cooled down.

Model parameters related to heat conduction and cure kinetics are estimated in two steps. First, the heat conduction part of the model is verified independent of the cure kinetics model. This is achieved by estimating the heat convection constant considering the given thermal properties of the composite laminate and the second set of temperature measurements (described in the above paragraph). The heat conduction part of the model along with the associated boundary condition

is given in equation (6) below, which are obtained by reducing the process model equations (1-5).

$$\rho c_p \frac{\partial T(z,t)}{\partial t} = \frac{\partial}{\partial z}\left(k_z \frac{\partial T(z,t)}{\partial z}\right) \tag{6a}$$

$$-k_z \frac{\partial T(0,t)}{\partial z} = h\left(T(0,t)-T_\infty\right) \tag{6b}$$

$$\frac{\partial T(l,t)}{\partial z} = 0 \tag{6c}$$

$$T(z,0) = T_0(z) \tag{6d}$$

Because of some heat loss in the insulation material, the second boundary condition (6c) may not be a good model of the insulation. To account for the loss of heat energy in the insulation material, either another conduction simulation using thermal properties of insulation material is required or it may be modeled by another convective boundary condition[12]. In this paper, the first one is adopted by simulating the coupled heat conduction model (PDEs) of composite laminate (6) and insulation material of thickness 22 mm. The thermal properties (density, heat capacity and thermal conductivity) are assumed to be independent of temperature and considered as constant parameters throughout the analysis. For the simulation, the PDEs in (6) are first transformed to a set of ODEs using a central-in-space finite difference method. Then, the set of ODEs is solved forward-in-time using Euler's method.

Given the average thermal properties of composite laminate that constitutes 40% fiber and 60% resin, the heat convection constant at the top surface was estimated using constrained optimization (e.g. via the matlab function FMINCON). In this work, we computed the convection constant that minimizes the square of the error between the temperature measurement and simulated results at the top and bottom boundaries of the composite sample. For the sample located at 80 mm from the UV lamp, the estimated a value for the convection constant is found to be 36 W/m^2 This value may change depending on the sample's distance from the lamp. At the last step, some of the cure kinetic parameters ($A_1, A_2, E_1, E_2 \& G$) are modified using the same optimization tool by comparing the simulation result for the complete process model (1-5) and the first set of temperature measurements.

The results that compare the simulated temperature evolution with the newly identified parameters and that of the measured temperature at the top ($z=0$) and bottom ($z=l$) surface of the composite laminate are plotted in Figures 5 a & b. Simulated cure state evolution at the top, middle and bottom of the sample are also plotted in Figure 5c. The complete set of parameters identified and used for the simulation of process model (1-5) is summarized in Table 1.
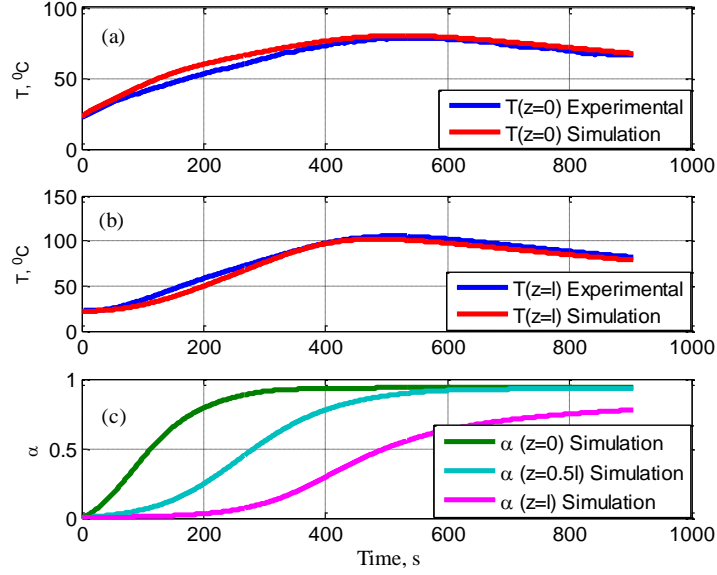
Figure 5: Comparison of simulated and measured temperature state: (a) top surface temperature, (b) bottom surface temperature; and (c) simulated cure state

In Figure 5, the process parameters identified based on these temperature measurements result in a good match of simulated temperature with that of the measured one. The corresponding cure state simulation in Figure 5c predicts a complete cure for layers at the top, and a maximum of 80 % conversion for the bottom. Although there was no direct measurement available to quantify the local cure conversion, for the cured sample, about 98% of the top surface average hardness value is measured at the bottom surface. This relative hardness value can be used to infer that the bottom cure conversion is closer to the top one. However, it should be expected that the complete cure values (critical cure level) for the top and bottom surfaces will differ as they are subjected to different UV intensities because of the differences of the diffusion-controlled effect[10]. Generally, the critical value of cure conversion due to diffusion-controlled effect is higher for higher UV intensities. In our simulation, we used the same parameters related to the diffusion-controlled effect ($x = 159.4 \& a_c = 0.92$) [10] throughout the sample depth. The limitations of this assumption need to be investigated further to quantify the diffusion-controlled effect on the exponentially decaying UV intensity along sample depth.

Table 1: Parameter Values Used in the Simulations

Parameter	Variable	Value
Density of composite	ρ	$1.69\,g/cm^3$
Specific heat of composite	c_p	$1.14\,J/g\,^oC$
Thermal conductivity of composite	k	$0.0026\,W/cm\,^oC$
Density of insulation material	ρ_i	$0.032\,g/cm^3$
Specific heat of insulation material	c_{pi}	$1.453\,J/g\,^oC$
Thermal conductivity of insulation material	k_i	$0.00024\,W/cm\,^oC$

Density of resin	ρ_r	$1.1\,g/cm^3$
Convective heat transfer	h	$0.0036\,W/cm^2\,{}^oC$
Polymerization enthalpy of resin	ΔH_r	$335\,J/g$
UV attenuation in the resin + fiber laminate	b_r	$6.5\,(cm)^{-1}$
UV attenuation due to photoinitiator	b_{PI}	$5\,(wt\%\,cm)^{-1}$
Activation energy	$E_1\,\&\,E_2$	$(43.2\,\&\,28.1)\,KJ/mol$
Photoinitiator concentration	S	$0.1\,wt\%$
Gas constant	R	$8.314\,J/mol\,K$
Pre-exponential rate constant	$A_1\,\&\,A_2$	$(4932\,\&\,25.7)\,(s)^{-1}$
Ambient temperature	T_∞	$22\,{}^oC$
Volume fraction of resin	v_r	0.6
Cure kinetics constant	G	2
Constants exponents	$p\,\&\,q$	$0.8\,\&\,0.7$
Absorptivity of UV radiation at surface	ϑ	0.85
Critical cure level	α_c	0.92
Diffusion constant	ξ	159.4

4. OPTIMAL LAYERING TIME CONTROL: RESULT AND DISCUSSION

The cure state simulated in Figure 5c shows large cure level deviations from the top to the bottom. For a 5 mm sample thickness, the top surface comes to complete cure in faster time and continues to over-cure (above, say a 90% target) while the bottom gets cured with attenuated UV intensity reaching the bottom. For larger sample thicknesses, this deviation will be higher and there may be little cure conversion at the bottom at all because of attenuation. To overcome these challenges, the composite laminate can be cured in a layer-by-layer process so that the inter-layer hold times can be optimized for minimal cure deviation at the final time (the detail derivations, numerical algorithm and extended discussion of this Stepped-Concurrent Curing(SCC) process are detailed in [7]). Here, we present some simulation results that compare the optimized final cure level deviation via the SCC process and one-shot concurrent curing (curing all layers at once) using the process model parameters experimentally verified in the previous sections of this paper. A cure level of 90% was set as a desired final cure level target. In the simulations, we considered a layer made from a 2-fiber ply laminate with an approximate thickness of 0.7 mm per layer. The UV intensity was set at 100 mW/cm^2. The results generated for a total sample thickness of 10.5 mm with total number of 15 layers are presented in Figures 6 a and b.
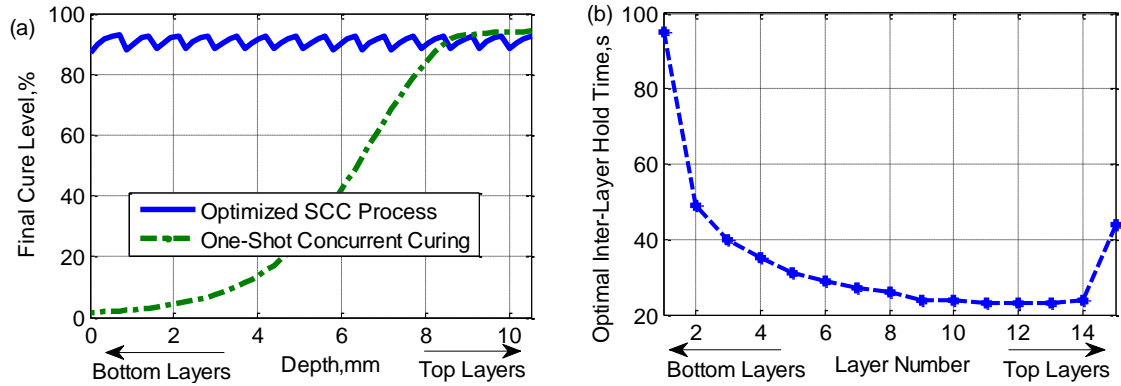
Figure 6: (a) Final cure level profile with SCC and one-shot curing; (b) Optimal inter-layer hold times

As shown in Figure 6a, for a one-shot concurrent curing, the cure deviation from the top to the bottom is very large. There is almost no cure for the bottom layers while the layers at the top come to a complete cure with overall curing duration of 517 seconds. On the other hand, with the SCC process, a minimum overall final cure deviation of less than 5% is achieved by optimizing the inter-layer hold times between layers. Referring to Figure 6b, the inter-layer hold time decreases as layers add on from the bottom then increases for the last top layers. The high hold times needed for the bottom layers are due to the anticipated large attenuations (via the model based optimization) as more layers are added on from the top. The high hold time for the last top layers is explained by the need for bringing the cure level to the desired level quickly from zero while other layers continues to cure from their partially cured state.

5. CONCLUSIONS

This paper discussed some experimental validations of a UV curing process mode1 for a polymer composite laminate. Measurements of UV transmission along the composite laminate with and without photoinitiator were used to estimate UV attenuation constants. Model parameters related with heat conduction and convection were determined using temperature measurements recorded after complete cure of composite laminate, where only these thermal effects remain. Finally, some of the cure kinetics parameters were estimated using in-situ temperature measurement during the curing process. The validated process model was then used to compute optimal inter-layer hold times for a stepped-concurrent curing process using the algorithm developed in [7]. Comparative curing process simulations for a thick composite laminate illustrated the advantages of the optimal SCC process over one-shot concurrent curing in minimizing cure-level deviations across all layers. In addition, with the optimal SCC process, the time needed to bring all layers to desired level of curing is shorter.

There are certain areas that need further investigation. First, no kinetic measurements have been conducted in this work. This would certainly improve the predictive ability of the process models and shall be pursued in the future. Next, the contributions and form of model for the diffusion-controlled effects in the curing process need further exploration.

6. ACKNOWLEDGEMENT

7. REFERENCES

[1] Y. Duan, J. Li, W. Zhong, R. G. Maguire, G. Zhao, H. Xie*, et al.*, "Effects of compaction and UV exposure on performance of acrylate/glass-fiber composites cured layer by layer," *Journal of Applied Polymer Science,* vol. 123, 2012, pp. 3799-3805.

[2] P. Compston, J. Schiemer, and A. Cvetanovska, "Mechanical properties and styrene emission levels of a UV-cured glass-fibre/vinylester composite," *Composite Structures,* vol. 86, 2008, pp. 22-26.

[3] D. Beziers, B. Capdepuy, and E. Chataignier, "Electron beam curing of composites," in *Developments in the Science and Technology of Composite Materials*, ed: Springer, 1990, pp. 73-78.

[4] A. Endruweit, M. S. Johnson, and A. C. Long, "Curing of composite components by ultraviolet radiation: A review," *Polymer composites,* vol. 27, 2006, pp. 119-128.

[5] A. Endruweit, W. Ruijter, M. S. Johnson, and A. C. Long, "Transmission of ultraviolet light through reinforcement fabrics and its effect on ultraviolet curing of composite laminates," *Polymer Composites,* vol. 29, 2008, pp. 818-829.

[6] H. Wenbin, L. Y. Tsui, and G. Haiqing, "A study of the staircase effect induced by material shrinkage in rapid prototyping," *Rapid Prototyping Journal,* vol. 11, 2005, pp. 82-89.

[7] A. Yebi and B. Ayalew, "Optimal Layering Time Control for Stepped-Concurrent Radiative Curing Process," *Journal of Manufacturing Science and Engineering,* vol. 137, 2015.

[8] S. Parthasarathy, S. C. Mantell, and K. A. Stelson, "Estimation, control and optimization of curing in thick-sectioned composite parts," *Journal of dynamic systems, measurement, and control,* vol. 126, 2004, pp. 824-833.

[9] A. Yebi and B. Ayalew, "A Hybrid Modeling and Optimal Control Framework for Layer-by-Layer Manufacturing Process," in *submitted to American Control Conference* Chicago, IL, 2015.

[10] P. Bártolo, "Optical approaches to macroscopic and microscopic engineering," PhD Dissertation,University of Reading, 2001.

[11] M. F. Perry and G. W. Young, "A mathematical model for photopolymerization from a stationary laser light source," *Macromolecular theory and simulations,* vol. 14, 2005, pp. 26-39.

[12] E. D.Bryant, "Development and verification of a thermal model for curved-layer laminated object manufacturing of polymer matrix composites," Master Thesis, University of Dayton, 1999.